

Wavevector- and frequency-dependent collective modes in one-component rare hot quantum and classical plasmas

This article has been downloaded from IOPscience. Please scroll down to see the full text article.

1995 J. Phys.: Condens. Matter 7 8405

(<http://iopscience.iop.org/0953-8984/7/44/009>)

View [the table of contents for this issue](#), or go to the [journal homepage](#) for more

Download details:

IP Address: 171.66.16.151

The article was downloaded on 12/05/2010 at 22:23

Please note that [terms and conditions apply](#).

Wavevector- and frequency-dependent collective modes in one-component rare hot quantum and classical plasmas

S P Tewari†, Hira Joshi and Kakoli Bera

Department of Physics and Astrophysics, University of Delhi, Delhi 110007, India

Received 10 August 1994, in final form 28 December 1994

Abstract. An analytical expression for the complex dielectric function $\varepsilon^Q(k, \omega) = \varepsilon_1^Q(k, \omega) + i\varepsilon_2^Q(k, \omega)$ for a one-component quantum hot rare plasma, valid for all values of the wavevector k and angular frequency ω , has been obtained using the two-particle quantum distribution function. It contains terms of all orders in \hbar^2 and reduces to $\varepsilon^{cl}(k, \omega)$, suggested earlier by us, when Planck's constant $\hbar = 0$. $\varepsilon_1^Q(k, \omega)$ yields a convergent value for $(\omega/kv) \gg 1$, unlike that given by the Green function formalism, when a large number of terms in the series are summed (V being the thermal velocity).

Expressions for the dynamic structure factors $S^Q(k, \omega)$ and $S^Q(k, \omega = 0)$ and the static structure factor $S^Q(k)$ have been obtained which reduce to the corresponding classical expressions when $\hbar = 0$.

Computations for one-component quantum and classical plasmas in an n-doped semiconductor having an electron density of $3.9 \times 10^{18} \text{ cm}^{-3}$ at 297 K have been made. $\varepsilon_1^Q(k, \omega)$, $\varepsilon_2^Q(k, \omega)$, $S^Q(k, \omega)$, etc. turn out to be quite different from the corresponding classical functions when $\hbar k/mV > 1$ (m being the mass of the mobile component). $S^Q(k, \omega)$, the singularity of which represents the collective mode, shows a smaller peak and its width is much broader in comparison with that of the corresponding $S^{cl}(k, \omega)$. The quantum-mechanical nature of the plasma thus introduces a sort of disorder in the plasma.

1. Introduction

A one-component rare plasma occurs in various physical situations such as the ionosphere, intergalactic space and doped semiconductors at appropriate density and temperatures. In such a plasma, only one component is mobile while the other is taken to be static and is essential for maintaining the charge neutrality of the plasma. The plasma is in thermodynamic equilibrium at a finite temperature (hot plasma); therefore, its collective modes are wavevector dependent [1, 2]. The complete dynamical information about such a system is contained in the frequency $\nu (= \omega/2\pi)$ and wavevector $|k|$ -dependent (where $|k| = 2\pi/\lambda$ with λ the wavelength and ω the angular frequency) complex dielectric function $\varepsilon(k, \omega)$, of the plasma. The real part of the dielectric function with put equal to zero and solved yields the collective modes of the plasma [2]. The imaginary part represents the damping of these modes. The plasma exhibits well defined collective modes when the damping is small.

Collective modes of the plasma can also be determined from the singularities of the dynamical structure factor $S(k, \omega)$, which can be obtained from the response function $1/\varepsilon(k, \omega)$ using the fluctuation–dissipation theorem [2, 6].

† Author to whom correspondence should be addressed.

When the mobile component forms a rare gas, there is hardly any interparticle interaction and one can use the Maxwellian distribution function for its momentum in the evaluation of $\varepsilon(k, \omega)$ [3–5]. In such a study, it is assumed that the mean interparticle distance $2r_s$, (r_s being the radius of the sphere assigned to each particle; $r_s = (3n/4\pi)^{1/3}$ where n is the number density of particles) is very large in comparison with the thermal de Broglie wavelength λ_{th} ($= h/\sqrt{2mk_B T}$ where h is the Planck constant, m the mass of the mobile component, k_B the Boltzmann constant and T the temperature of the rare gas); therefore, the plasma is referred to as a one-component classical rare hot plasma (OCCRHP). However, there may be a situation in practice where such an approximation is not valid; one will, therefore, have to take into account this quantum-mechanical effect. In this case the plasma is referred to as a one-component quantum-mechanical rare hot plasma (OCQRHP) or weakly degenerate rare plasma in contrast to the case of a metal where the plasma is dense and strongly degenerate [7, 8]. The general complex dielectric function for such a plasma has hardly been investigated. It is, therefore, worthwhile to study and compare the wavevector- and frequency-dependent collective modes in an OCQRHP and an OCCRHP. In addition, knowledge of the full $\varepsilon(k, \omega)$ is essential to evaluate various physical quantities such as the loss of energy of a charged particle [7, 9] passing through it and the build-up of the mobile component about a finite mass charged impurity [5] which may also yield the positron annihilation rate [10] in the plasma where electrons are the mobile particles. In this paper we have derived an explicit expression for an OCQRHP using the two-particle quantum distribution function, studied its various cases and investigated the wavevector-dependent collective modes for both an OCQRHP and an OCCRHP.

In section 2 we give different mathematical formulations. The results and discussion are given in section 3, followed by the conclusions in section 4.

2. Mathematical formalism

2.1. Dielectric function

The expression for the wavevector- and angular-frequency-dependent dielectric function $\varepsilon^Q(k, \omega)$, for a one-component quantum plasma, in terms of two-particle quantum distribution functions $f_{\pm}(k, \omega)$ is given as follows [11]:

$$\varepsilon(k, \omega) = 1 + \frac{2\pi i}{h} [f_+(k, \omega) - f_-(k, \omega)]. \quad (1)$$

The expression for the quantum two-particle distribution function when the single-particle momentum distribution function $f_0(p)$ is taken to be Maxwellian (i.e. $f_0(p) = A \exp(-p^2/2mk_B T)$) as is appropriate for the one-component rare hot plasma is given as follows [11, 12]:

$$f_{\pm}(k, \omega) = \frac{1}{2\pi i} \frac{4\pi n e^2}{k^2} \int \frac{dp}{(\omega - \mathbf{k} \cdot \mathbf{p}/m + i\varepsilon)} f\left(p \pm \frac{hk}{2}\right) \quad (2)$$

where e and p are the charge and the linear momentum of the electron respectively. Substituting for $f_{\pm}(k, \omega)$ from equation (2) in equation (1) and solving for the limit $\hbar = 0$, it can be shown that equation (1) reduces to the following well known classical expression obtained from the collisionless linearized Boltzmann transport equation [4]:

$$\varepsilon^{cl}(k, \omega) = 1 + \frac{4\pi e^2}{k^2} \mathbf{k} \cdot \int \frac{\partial f_0(p)}{\partial p} \frac{dp}{(\omega - \mathbf{k} \cdot \mathbf{p}/m + i\varepsilon)}. \quad (3)$$

Making use of the Maxwellian momentum distribution function in equation (2), and the Dirac identity

$$\frac{1}{x + i\epsilon} = P\left(\frac{1}{x}\right) - i\pi\delta(x) \quad (4)$$

one can solve for the imaginary part of $f_{\pm}(k, \omega)$ after assuming \mathbf{k} to be parallel to the z axis, without any loss of generality, to obtain the following:

$$\begin{aligned} \text{Im } f_{\pm}(k, \omega) &= \sqrt{\frac{2\pi m n e^2}{k_B T}} \frac{1}{k^3} \exp\left(-\frac{\hbar^2 k^2}{8mk_B T}\right) \exp\left(-\frac{m\omega^2}{2k^2 k_B T}\right) \\ &\times \left[\exp\left(\frac{\hbar\omega}{2k_B T}\right) - \exp\left(-\frac{\hbar\omega}{2k_B T}\right) \right]. \end{aligned} \quad (5)$$

The value of A is evaluated using the following sum rule:

$$\int_0^{\infty} \omega \text{Im}[\epsilon(k, \omega)] d\omega = \frac{\pi}{2} \omega_p^2 \quad (6)$$

where $\omega_p (= \sqrt{4\pi n e^2/m})$ is the angular plasma frequency of the electrons. Using equations (4) and (2) one obtains for the real part of $f_{\pm}(k, \omega)$

$$\text{Re}[f_{\pm}(k, \omega)] = \frac{4\pi n e^2 m^2 k_B T A}{k^3 i} \exp\left(-\frac{\hbar^2 k^2}{8mk_B T}\right) \int_{-\infty}^{\infty} \frac{dp_z}{\omega - \omega'} \exp\left[-\left(\frac{p_z^2 \pm \hbar k p_z}{2mk_B T}\right)\right] \quad (7)$$

where $\omega' = k p_z/m$. Using the transformations

$$x^2 = \frac{m\omega'^2}{2k^2 k_B T} \quad y^2 = \frac{m\omega^2}{2k^2 k_B T}$$

to simplify equation (7), one obtains

$$\text{Re}[f_{\pm}(k, \omega)] = \frac{4\pi n e^2 m^2 k_B T A}{k^3 i} \int_{-\infty}^{\infty} \frac{dx}{y - x} \exp\left[-\left(x \pm \frac{D}{2}\right)^2\right] \quad (8)$$

with $D = k\lambda_{th}$. Equation (8) can be rewritten as

$$\begin{aligned} \text{Re } f_{\pm}(k, \omega) &= \frac{4\pi n e^2}{k^3 i} \left(\frac{m}{k_B T}\right)^{1/2} \frac{1}{\sqrt{2\pi}} \left[\Phi\left\{\left(\frac{m\beta}{2}\right)^{1/2} \left(\frac{\omega}{k} + \frac{\hbar k}{2m}\right)\right\} \right. \\ &\left. - \Phi\left\{\left(\frac{m\beta}{2}\right)^{1/2} \left(\frac{\omega}{k} - \frac{\hbar k}{2m}\right)\right\} \right] \end{aligned} \quad (9)$$

where $\beta = 1/k_B T$ and

$$\Phi(z) = \pi^{-1/2} P \int_{-\infty}^{\infty} dt \frac{\exp(-t^2)}{z - t}.$$

After solving the principal value integral occurring in (8) one can write the complete dielectric function for the OCQRHP as

$$\begin{aligned} \epsilon^Q(k, \omega) &= 1 + \frac{\omega_p^2}{\sqrt{2}k^2 V^2} \frac{mV}{\hbar k} \left[\left[\exp\left[-\left(\frac{\omega}{\sqrt{2}kV} + \frac{\hbar k}{2\sqrt{2}mV}\right)^2\right] \left(\frac{\omega}{\sqrt{2}kV} + \frac{\hbar k}{2\sqrt{2}mV}\right) \right. \right. \\ &\left. \left. \times \left\{ 1 + \frac{1}{3} \left(\frac{\omega}{\sqrt{2}kV} + \frac{\hbar k}{2\sqrt{2}mV}\right)^2 + \dots \right\} - \exp\left[-\left(\frac{\omega}{\sqrt{2}kV} - \frac{\hbar k}{2\sqrt{2}mV}\right)^2\right] \right] \right] \end{aligned}$$

$$\begin{aligned} & \times \left(\frac{\omega}{\sqrt{2}kV} - \frac{hk}{2\sqrt{2}mV} \right) \left\{ 1 + \frac{1}{3} \left(\frac{\omega}{\sqrt{2}kV} - \frac{hk}{2\sqrt{2}mV} \right)^2 + \dots \right\} \\ & + i\sqrt{\frac{\pi}{2}} \frac{1}{\sqrt{2}} \exp[-(\omega^2/2k^2V^2)] \\ & \times \left\{ \exp \left[-\frac{1}{8} \left(\frac{hk}{mV} \right)^2 \right] (\exp(h\omega/2k_B T) - \exp(-h\omega/2k_B T)) \right\} \end{aligned} \quad (10)$$

$$\varepsilon^Q(k, \omega) = \varepsilon_1^Q(k, \omega) + i\varepsilon_2^Q(k, \omega) \quad (11)$$

where $V (= \sqrt{k_B T/m})$ is the thermal velocity. Equation (10) is the full quantum wavevector and frequency-dependent dielectric function of a one-component rare hot plasma.

We now consider the particular cases of $\varepsilon^Q(k, \omega)$ given by equation (10).

When $\omega = 0$, $\varepsilon_2^Q(k, \omega) = 0$ and $\varepsilon_1^Q(k, \omega)$ reduces to the following:

$$\varepsilon_1^Q(k, 0) = 1 + \frac{\sqrt{2}\omega_p^2 m}{Vhk^3} D \exp\left(-\frac{D^2}{4}\right) \left[1 + \frac{1}{3} \left(\frac{D}{2}\right)^2 + \frac{1}{10} \left(\frac{D}{2}\right)^4 + \dots \right] \quad (12)$$

which is the same as

$$\varepsilon_1^Q(k, 0) = 1 + \frac{\omega_p^2}{k^2 V^2} \exp\left(-\frac{D^2}{4}\right) \int_0^1 \exp\left(\frac{D^2 x^2}{4}\right) dx \quad (13)$$

in agreement with the results obtained earlier [12, 14, 15]. When $h = 0$, equation (13) reduces to the well known classical expression [5, 13] given as follows:

$$\varepsilon_1^{cl}(k, 0) = 1 + \frac{\omega_p^2}{k^2 V^2}. \quad (14)$$

When $h = 0$, $\varepsilon^Q(k, \omega)$ reduces to $\varepsilon^{cl}(k, \omega)$, which can also be seen by putting equation (10) in the following alternative form:

$$\begin{aligned} \varepsilon^Q(k, \omega) = \varepsilon^{cl}(k, \omega) + h^2 & \left\{ \frac{\omega_p^2}{2m^2 V^4} \left[-\frac{1}{6} + \frac{2}{3} \left(\frac{\omega^2}{2k^2 V^2} \right) - \dots + \dots \right] \right. \\ & + \frac{i\sqrt{\pi}}{8} \frac{\omega_p^2}{m^2 V^4} \left[-\frac{\omega}{\sqrt{2}kV} + \frac{5}{3} \left(\frac{\omega^2}{2k^2 V^2} \right)^{3/2} - \dots + \dots \right] \left. \right\} \\ & + h^4 \left\{ \frac{\omega_p^2 k^2}{4m^4 V^6} \left[-\frac{1}{60} - \frac{1}{10} \left(\frac{\omega^2}{2k^2 V^2} \right) - \dots \right] \right. \\ & + \frac{i\sqrt{\pi}}{128} \frac{\omega_p^2}{m^4 V^6} \left[-\frac{\omega}{\sqrt{2}kV} - 7 \left(\frac{\omega^2}{2k^2 V^2} \right)^2 - \dots \right] \left. \right\} + O(h^6) + O(h^8) + \dots \end{aligned} \quad (15)$$

where

$$\varepsilon^{cl}(k, \omega) = \varepsilon_1^{cl}(k, \omega) + i\varepsilon_2^{cl}(k, \omega) \quad (16)$$

with

$$\begin{aligned} \varepsilon_1^{cl}(k, \omega) = 1 + \frac{\omega_p^2}{k^2 V^2} - \frac{\omega_p^2}{k^2 V^2} \frac{\omega^2}{k^2 V^2} \exp\left(-\frac{\omega^2}{2k^2 V^2}\right) \\ \times \left[1 + \frac{1}{3} \left(\frac{\omega^2}{2k^2 V^2} \right) + \frac{1}{10} \left(\frac{\omega^2}{2k^2 V^2} \right)^2 + \dots \right] \end{aligned} \quad (17)$$

and

$$\varepsilon_2^{cl}(k, \omega) = \sqrt{\frac{\pi}{2}} \frac{\omega_p^2}{k^2 V^2} \frac{\omega}{kV} \exp\left(-\frac{\omega^2}{2k^2 V^2}\right). \quad (18)$$

These are the well known expressions for the real and imaginary parts of the classical dielectric function [3, 5].

Thus, $\varepsilon^Q(k, \omega)$ (equation (10)) can be viewed as a generalization of $\varepsilon^{cl}(k, \omega)$ (equation (16)), when the thermal de Broglie wavelength of the electrons is not zero but finite. Further, as long as the mobile component, i.e. electrons in the present consideration, follow the Maxwellian distribution of momentum, equation (10) incorporates the full quantum-dynamical behaviour of the system, i.e. it contains terms to all orders in \hbar^2 , \hbar being the Planck constant.

Some of the studies on the equation of state of the fully ionized quantum plasma indicate the presence of a $\Lambda_e^2 \ln \gamma_e$ singularity [16] where $\Lambda_e = Z_e^2 e^2 / \lambda_D k_B T$ and $\gamma_e = \lambda_{ih} / \lambda_D$ where λ_D is the Debye screening length and is given as $(4\pi n Z_e^2 e^2 / k_B T)^{-1/2}$, i.e. one has essentially a contribution of the form $\ln h$, which yields a singularity when $h = 0$. However, when one considers a plasma which is fully ionized and consists of an equal number of oppositely charged particles, just as the case under consideration, no singularity appears when $h = 0$ [16].

In the appendix we show that the expression for $\varepsilon^Q(k, \omega)$, i.e. equation (10) for the OCQRHP, is in agreement with the alternative Green function formalism (the starting point of which is a strongly degenerate dense plasma), under appropriate conditions for a quantum hot rare plasma. Since the complex dielectric function has both k and ω dependences, this can be used to study various physical processes which are dependent on the full $\varepsilon(k, \omega)$ such as light scattering, positron annihilation rate and AC conductivity, as has also been alluded to earlier.

2.2. Dynamical structure factor

The general expression for $S(k, \omega)$ using the linear response function $[\varepsilon(k, \omega)]^{-1}$ and fluctuation-dissipation theorem is given as follows [2, 6]:

$$S(k, \omega) = -\frac{n}{\pi \omega} \frac{k^2}{k_-^2} \text{Im} \left[\frac{1}{\varepsilon(k, \omega)} \right] \quad (19)$$

where $k_-^2 = 1/\lambda_D^2$, λ_D is the Debye screening length. For the OCQRHP, it can be written as

$$S^Q(k, \omega) = \frac{n}{\pi \omega} \frac{k^2}{k_-^2} \frac{\varepsilon_2^Q(k, \omega)}{[(\varepsilon_1^Q(k, \omega))^2 + (\varepsilon_2^Q(k, \omega))^2]} \quad (20)$$

where $\varepsilon_1^Q(k, \omega)$ and $\varepsilon_2^Q(k, \omega)$ are given by equations (10) and (11). Substituting for $\varepsilon_1^Q(k, \omega)$ and $\varepsilon_2^Q(k, \omega)$ in equation (20), one gets $S^Q(k, \omega)$ as

$$S^Q(k, \omega) = \frac{n}{\sqrt{2\pi}} \frac{1}{[(\varepsilon_1^Q(k, \omega))^2 + (\varepsilon_2^Q(k, \omega))^2]} P(k, \omega) \quad (21)$$

with

$$P(k, \omega) = \frac{mV}{\hbar k} \frac{1}{\omega} \left\{ \exp \left[-\left(\frac{\omega}{\sqrt{2}kV} - \frac{\hbar k}{2\sqrt{2}mV} \right)^2 \right] - \exp \left[-\left(\frac{\omega}{\sqrt{2}kV} + \frac{\hbar k}{2\sqrt{2}mV} \right)^2 \right] \right\}. \quad (22)$$

When $\omega = 0$, the quantum expression for the zero-frequency dynamic structure factor $S^Q(k, 0)$ is given as follows:

$$S^Q(k, 0) = \frac{n}{\sqrt{2\pi}} \frac{1}{\varepsilon_1^2(k, 0)} \frac{1}{kV} \exp\left(-\frac{\hbar^2 k^2}{8m^2 V^2}\right) \quad (23)$$

where $\varepsilon_1^Q(k, 0)$ is given by equation (12).

The static structure factor $S(k)$ can be written as

$$S(k) = \int_{-\infty}^{\infty} S(k, \omega) d\omega. \quad (24)$$

Using equation (19) in the Kramers–Kronig relation

$$\operatorname{Re}\left[\frac{1}{\varepsilon(k, \omega)} - 1\right] = \frac{1}{\pi} \int_{-\infty}^{\infty} P\left(\frac{1}{\omega' - \omega}\right) \operatorname{Im}\left(\frac{1}{\varepsilon(k, \omega')}\right) d\omega' \quad (25)$$

the expression for the quantum static structure factor $S^Q(k)$ can be obtained as

$$S^Q(k) = -\frac{k^2}{k_-^2} \left[\frac{1}{\varepsilon_1^Q(k, 0)} - 1 \right] \quad (26a)$$

which is equal to

$$S^Q(k) = \frac{C(k\lambda_{th})k^2}{k^2 + k_-^2 C(k\lambda_{th})} \quad (26b)$$

where equation (12) for $\varepsilon_1^Q(k, 0)$ is written as

$$\varepsilon_1^Q(k, 0) = 1 + \frac{k_-^2}{k^2} C(k\lambda_{th}). \quad (27)$$

2.2.1. Classical cases. When $\hbar = 0$, $\varepsilon_1^Q(k, \omega)$ and $\varepsilon_2^Q(k, \omega)$ reduce to their corresponding classical parts as given by equations (15)–(18).

Similarly, when $\hbar = 0$, the quantum expressions for $S^Q(k, \omega)$, $S^Q(k, 0)$ and $S^Q(k)$ all reduce to the corresponding classical expressions given as follows:

$$S^{cl}(k, \omega) = \frac{n}{\pi} \frac{k^2}{k_-^2} \frac{\varepsilon_2^{cl}(k, \omega)}{[(\varepsilon_1^{cl}(k, \omega))^2 + (\varepsilon_2^{cl}(k, \omega))^2]} \quad (28)$$

$$S^{cl}(k, 0) = \frac{n}{\sqrt{2\pi}} \frac{1}{(1 + k_-^2/k^2)^2} \frac{1}{kV} \quad (29)$$

and

$$S^{cl}(k) = k^2/(k^2 + k_-^2). \quad (30)$$

3. Results and discussions

Equation (10) is the full wavevector- and frequency-dependent complex dielectric function for the OCQRHP.

This expression is different from that derived for the dense electron gas in metals [7] which even in the classical limit, when the Fermi–Dirac distribution function goes over to Maxwellian, is accompanied by the local field correction factor $G(k)$. In the random-phase approximation $G(k) = 0$ and, when the appropriate classical limit is taken, the expression for $\varepsilon(k, \omega)$ turns out to be the same [8] as obtained by others [15] earlier. However, this

work, although correct for $\omega/kV \ll 1$, yields a divergent unphysical result when $\omega/kV \gg 1$ (appendix). Such is not the case in the present formalism. Equation (10) reduces correctly to the case of a classical plasma given by equations (17) and (18), representing the real and imaginary parts of the dielectric function, when the Planck constant \hbar is put equal to zero. As is evident from equations (10) and (16), the real part of $\varepsilon(k, \omega)$ contains a series, which has to be properly evaluated for a mode in a given physical system, specified by its density, temperature and mass. For example, in the case of $\varepsilon_1^{cl}(k, \omega)$ for small values of ω/kV , it reaches a convergent result even for small number N of terms but, as ω/kV increases, one faces a convergence problem. It is only when the number of terms is taken to be quite large (sometimes as large as 160 terms) that one obtains a convergent result. This problem of convergence is less acute in the case of $\varepsilon_1^Q(k, \omega)$. No such difficulty is encountered in the evaluation of $\varepsilon_2(k, \omega)$, in both cases, as it is an exponential function in $[-(\omega/\sqrt{2kV})^2]$. Keeping this in mind, one can study the various properties of the plasma dependent on k and ω .

It may be noted that $\varepsilon^Q(k, \omega)$ and $\varepsilon^{cl}(k, \omega)$ given by equations (10) and (16), respectively, are valid for all values of ω/kV and reduce correctly to the respective cases when $\omega/kV \ll 1$ and $\omega/kV \gg 1$. For $\omega/kV \ll 1$, $\varepsilon_1^{cl}(k, \omega)$ approaches $[1 + \omega_p^2/k^2V^2]$ [2] and, for $\omega/kV \gg 1$, it approaches $(1 - \omega_p^2/k^2V^2)$ [2]. Similarly, for $\omega/kV \ll 1$ [15], $\varepsilon_1^Q(k, \omega)$ reduces to

$$\varepsilon_1^Q(k, \omega) = 1 + \frac{\omega_p^2 m}{\sqrt{2} V \hbar k^3} \left[2 \left(\frac{\omega}{\sqrt{2} k V} + \frac{\hbar k}{2\sqrt{2} m V} \right) \left\{ 1 + \frac{1}{3} \left(\frac{\omega}{\sqrt{2} k V} + \frac{\hbar k}{2\sqrt{2} m V} \right)^2 + \dots \right\} - 2 \left(\frac{\omega}{\sqrt{2} k V} - \frac{\hbar k}{2\sqrt{2} m V} \right) \left\{ 1 + \frac{1}{3} \left(\frac{\omega}{\sqrt{2} k V} - \frac{\hbar k}{2\sqrt{2} m V} \right)^2 + \dots \right\} \right]$$

and, for $\omega/kV \gg 1$, it approaches

$$\varepsilon_1^Q(k, \omega) = 1 + \sqrt{2} \frac{\omega_p^2 m}{V \hbar k^3} \left[\exp \left[- \left(\frac{\omega}{\sqrt{2} k V} + \frac{\hbar k}{2\sqrt{2} m V} \right)^2 \right] \left(\frac{\omega}{\sqrt{2} k V} + \frac{\hbar k}{2\sqrt{2} m V} \right) \times \left\{ 1 + \frac{1}{3} \left(\frac{\omega}{\sqrt{2} k V} + \frac{\hbar k}{2\sqrt{2} m V} \right)^2 + \dots \right\} - \exp \left[- \left(\frac{\omega}{\sqrt{2} k V} - \frac{\hbar k}{2\sqrt{2} m V} \right)^2 \right] \times \left(\frac{\omega}{\sqrt{2} k V} - \frac{\hbar k}{2\sqrt{2} m V} \right) \left\{ 1 + \frac{1}{3} \left(\frac{\omega}{\sqrt{2} k V} - \frac{\hbar k}{2\sqrt{2} m V} \right)^2 + \dots \right\} \right].$$

We shall discuss these further, later.

In order to study the collective modes of the plasma, one demands that $\varepsilon_1(k, \omega) = 0$. For example, in earlier studies [1], the collective modes for the OCCRHP have been determined in the region $\omega/kV \gg 1$ using the approximate $\varepsilon_1(k, \omega)$ given as follows:

$$\varepsilon_1(k, \omega) = 1 - \frac{\omega_p^2}{\omega^2} \left(1 + \frac{3k^2V^2}{\omega^2} \right). \quad (31)$$

One obtains rather easily the approximate ω versus k relationship, i.e.

$$\omega^2 = \omega_p^2 \left(1 + \frac{3k^2}{k_-^2} \right). \quad (32)$$

To study collective modes of plasma for any value of ω/kV , one will have to solve equation (17) for its zeros. This involves solution of a polynomial of very high degree in $(\omega/kV)^2$. (The polynomial structure of the equation for any value of (ω/kV) can also

be seen by shifting the exponential.) It, therefore, becomes quite difficult to obtain collective modes using this approach.

As has been emphasized in section 2, collective modes are also given by singularities of $S(k, \omega)$. For the quantum and classical cases, therefore, these can be determined by finding numerically the singularities of equations (20) and (28), respectively. $S(k, \omega)$ satisfies the sum rule given by equation (24), which can be determined using the computed $S(k, \omega)$ and also using other algebraic forms given by equation (26b) for the quantum case and equation (30) for the classical case. The sum rule, which is essentially the static structure factor of the plasma, thus determined in two different ways ensures the correctness of the calculations. Further, the collective modes thus determined can be used in the expression for $\epsilon_1(k, \omega)$ to check its approach to zero. This procedure further confirms the correct determination of the collective modes. One can also check their correctness for $\omega = 0$, by determining the values of $S^Q(k, 0)$ and $S^{cl}(k, 0)$ given by equations (23) and (29) for quantum and classical plasmas, respectively, with the corresponding calculated values using $S^Q(k, \omega = 0)$ and $S^{cl}(k, \omega = 0)$.

The collective mode for a given k is said to be well defined when $S(k, \omega)$ shows an extremely sharp increase near a given frequency. The full width at half-maximum represents the damping of the modes. (In the case of monatomic liquids [19] this width represents the extent of disorder. $S(k, \omega)$ in the case of the corresponding crystal is a delta function [18].) To illustrate these points we consider an example of an OCCRHP which can be easily obtained in an n-type semiconductor [17]. The mobile particles in this case are electrons. The plasma is considered to be at the temperature 297 K, having an electron number density of $3.9 \times 10^{18} \text{ cm}^{-3}$ which corresponds to $r_s \simeq 39.42 \text{ \AA}$. The plasma frequency ω_p is equal to 0.088 eV, where the mass of the mobile component is equal to $0.7m_e$ (m_e is the mass of an electron). We have evaluated $\epsilon_1^{cl}(k, \omega)$ using equation (17), taking $k = 4.25 \times 10^6 \text{ cm}^{-1}$ which corresponds to $\lambda = 3.75r_s$. In figure 1 is shown the variation in $\epsilon_1^{cl}(k, \omega)$ with different values of ω/kV . As discussed earlier, $\epsilon_1^{cl}(k, \omega)$ yields different values for large values of ω/kV when the number of terms taken is different. For instance, as shown in figure 1, when $\omega/kV = 6$, one gets $\epsilon_1^{cl}(k, \omega) \simeq 5.8$ when $N = 18$, which reduces to 0.6 when $N = 35$ and converges to 0.5 when $N = 50$ and remains so for larger values of N . Thus, for this case the converged result is obtained when $N \geq 50$. Similarly for ω/kV equal to, say, 9 the converged result is obtained when N is around 100. When ω/kV is still larger, equal to, say, 15 (not shown in the figure), then convergence is obtained at around $N = 160$. Correctly computed values of $\epsilon_1^{cl}(k, \omega)$ are shown in figure 1 by the full curve. It has a value around 16.24 for $\omega/kV = 0$ which decreases as ω/kV increases. It becomes negative when ω/kV lies between 1.4 and 4.25 with a dip at $\omega/kV \simeq 2.05$. For ω/kV greater than 4.25, its value slowly increases and tends to one for larger values of ω/kV . The variation in $\epsilon_1^{cl}(k, \omega)$ when $\omega/kV \ll 1$ is exactly the same as that given by Ichimaru [2]. Similarly, when $\omega/kV \gg 1$, the results are again the same as that given by Ichimaru [2], which corresponds to the expression

$$\epsilon_1(\omega) = 1 - \frac{\omega_p^2}{\omega^2} \quad (33)$$

an expression which is independent of k and is the well known Drude model. Therefore, the analytical expression for $\epsilon_1^{cl}(k, \omega)$ given by the equation (17) for a system yields correctly the values of $\epsilon_1^{cl}(k, \omega)$ for any value of ω/kV .

Now we relax the condition that the plasma is classical and incorporate its quantum-mechanical nature. For the system under consideration $\lambda_{rh} \simeq 91.6 \text{ \AA}$, which is comparable with $2r_s$. We, therefore, now study $\epsilon^Q(k, \omega)$ of the plasma using equation (10). From

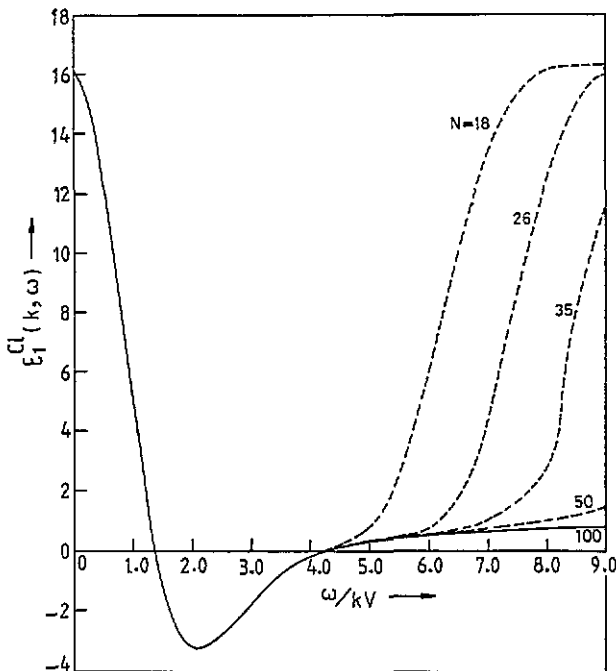


Figure 1. Variation in the real part of classical, wavevector- and frequency-dependent dielectric function, given by equation (17) with the angular frequency ω expressed in terms of kV , for wavevector $k = 4.25 \times 10^6 \text{ cm}^{-1}$ in the OCCRHP, having the number density equal to $3.9 \times 10^{18} \text{ cm}^{-3}$, of the mobile electrons, at temperature $T = 297 \text{ K}$. $V (= \sqrt{k_B T/m})$, k_B is the Boltzmann constant and m is the mass of the electron taken to be $0.7m_e$. Broken curves represent the calculated values of $\varepsilon_1^{cl}(k, \omega)$ when the number N of terms in its evaluation using equation (17) are taken to be 18, 26, 35, 50 and 100. For $\omega/kV \leq 4$ the results are convergent for even smaller values of N (≈ 12).

equation (10) for $\varepsilon_1^Q(k, \omega)$, it is evident that the ratio $R (= hk/mV)$ may be chosen as a parameter to indicate the deviation of a system from the classical. When $R \rightarrow 0$, the system approaches the classical description and, as R increases, it exhibits more and more quantum-mechanical behaviour described by equations (11) and (10). In figure 2 are plotted $\varepsilon_1^Q(k, \omega)$ with ω/kV given by equations (11) and (10) for the plasma under consideration, for different values of R . When R is equal to 0.0001, the values of $\varepsilon_1^Q(k, \omega)$ correspond closely to the classical variation in $\varepsilon_1^{cl}(k, \omega)$ as calculated from equation (17) and shown in figure 2. As R increases, $\varepsilon_1^Q(k, \omega)$ becomes increasingly different from $\varepsilon_1^{cl}(k, \omega)$, for different values of R equal to 1, 2, 3 and 5. While for $R = 1$ the difference between the two is slight, for $R = 3$ it is significant particularly for ω/kV lying between 0 and approximately 5, as is clear from the figure. For $R = 5$, the difference becomes more pronounced. The effect of increasing R results in a decrease in the value of $\varepsilon_1^Q(k, 0)$, its broadening for low values of ω/kV , a shift in the negative region to higher ω/kV -values and a decrease in the depth of the negative valley, as is evident from the figure. There is little difference between $\varepsilon_1^Q(k, \omega)$ and $\varepsilon_1^{cl}(k, \omega)$ for ω/kV greater than 6. Hence the difference between $\varepsilon_1^Q(k, \omega)$ and $\varepsilon_1^{cl}(k, \omega)$ is significant when ω/kV is small.

In figure 3 are plotted $\varepsilon_2^Q(k, \omega)$ given by equations (11) and (10) for different values of R together with $\varepsilon_2^{cl}(k, \omega)$ given by equation (18) with ω/kV . When $R = 0.0001$, $\varepsilon_2^Q(k, \omega)$

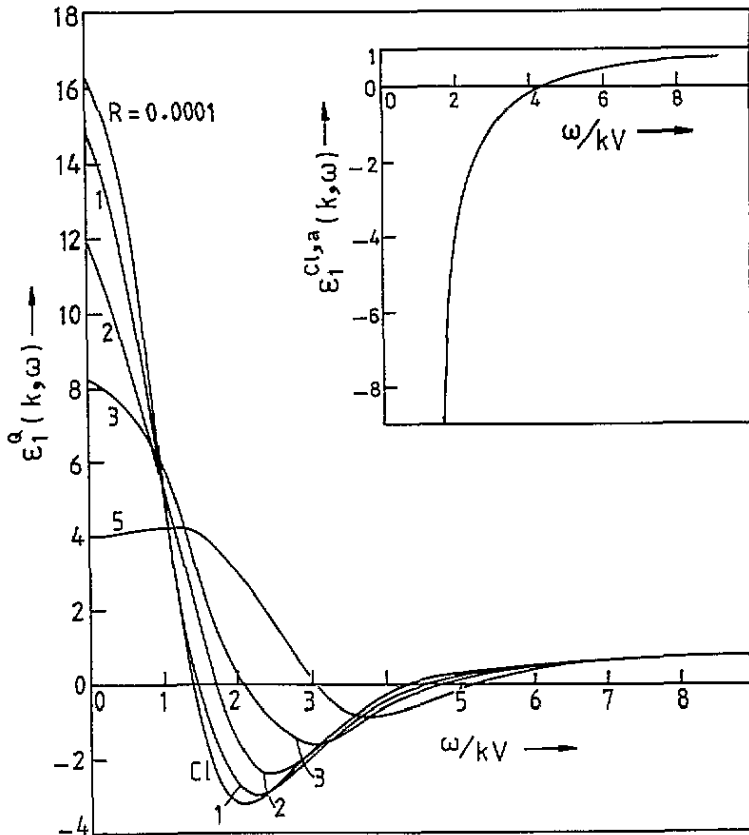


Figure 2. Variation in the real part of the quantum wavevector- and frequency-dependent dielectric function $\epsilon_1^Q(k, \omega)$ given by equation (10), with the angular frequency ω expressed in terms of kV , for $k = 4.25 \times 10^6 \text{ cm}^{-1}$, in the OCQRHP having the number density $n = 3.9 \times 10^{18} \text{ cm}^{-3}$ at temperature $T = 297 \text{ K}$, for different values of quantum parameter $R (= \hbar k/mV) = 0.0001, 1, 2, 3$ and 5 . h is the Planck constant. Variation in $\epsilon_1^Q(k, \omega)$ for $R = 0.0001$ corresponds very closely to that of classical $\epsilon_1(k, \omega)$. All results for $\epsilon_1^Q(k, \omega)$ correspond to the properly converged values of the series occurring in equation (10). The inset shows the variation in the classical approximate dielectric function $\epsilon_1^{cl,a}(k, \omega)$ calculated using equation (31) with ω/kV .

is very close to that calculated from $\epsilon_2^{cl}(k, \omega)$. As R increases, the difference between $\epsilon_2^Q(k, \omega)$ and $\epsilon_2^{cl}(k, \omega)$ increases, as shown in the figure. The effect of increasing R results in the broadening of the function, lessening of the peak values, shift in the peak values to higher ω/kV -values and rounding off of the peak values as evident from the figure. As R increases, while there is a decrease in Landau damping for small values of ω/kV , there is an increase in the damping for larger values of ω/kV in comparison with the Landau damping in the classical case as is clear from the figure. The extent of Landau damping is also more in the quantum-mechanical case in comparison with the corresponding classical situation.

We now turn to the study of collective modes in the system. We consider first the classical case. $S^{cl}(k, \omega)$ as the second inverse s^{-1} has been computed by making use of equation (28). The precaution that one has to take is to use correct values of $\epsilon_1^{cl}(k, \omega)$, as has been discussed earlier. For $k = 4.25 \times 10^6 \text{ cm}^{-1}$, the variation in $S^{cl}(k, \omega)$ with ω

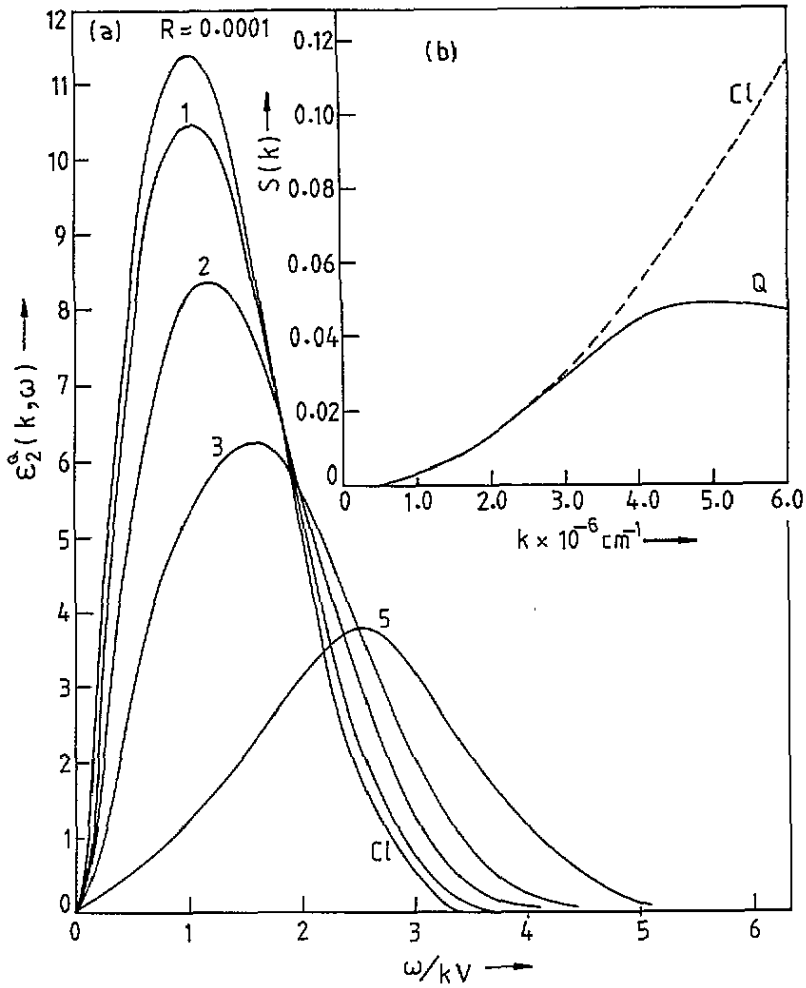


Figure 3. (a) Variation in the imaginary part of the quantum wavevector- and frequency-dependent dielectric function $\epsilon_2^0(k, \omega)$, given by equation (10) with ω/kV , for $k = 4.25 \times 10^6 \text{ cm}^{-1}$ in the OCQRHP having the number density $n = 3.9 \times 10^{18} \text{ cm}^{-3}$ at temperature $T = 297 \text{ K}$ for different values of quantum parameter $R = 0.0001, 1, 2, 3$ and 5 . Variation in $\epsilon_2^0(k, \omega)$ for $R = 0.0001$ corresponds very closely to that given by $\epsilon_2^{cl}(k, \omega)$. (b) Variation in the computed values of the static structure factor $S(k)$ of the one-component plasma for different values of wavevector k : ---, classical plasma; —, quantum plasma.

has been plotted in figure 4. There is a sharp peak for $\omega = 0.098 \text{ eV}$ which corresponds to a well defined collective oscillation in the system. For this mode, $\epsilon_1^{cl}(k, \omega)$ is nearly equal to zero when the number of terms in its polynomial is equal to 160. As $S^{cl}(k, \omega)$ is a symmetric function, we get exactly the same variation when ω goes to $-\omega$. The zeroth sum rule given by equation (24) using the calculated values of $S^{cl}(k, \omega)$ is found to agree with the calculations done using equation (30). Similarly $S^{cl}(k, \omega = 0)$ from the calculation of $S^{cl}(k, \omega)$ is found to agree with the calculated values using equation (29).

As the approximate expression for $\epsilon_1(k, \omega)$ given by (31) plotted in the inset of figure (2) is widely used, we have computed $S(k, \omega)$ for this case too and, in order to differentiate it from $S^{cl}(k, \omega)$ discussed so far, we denote it by $S^{cl,a}(k, \omega)$. The expression for $\epsilon_2(k, \omega)$ in

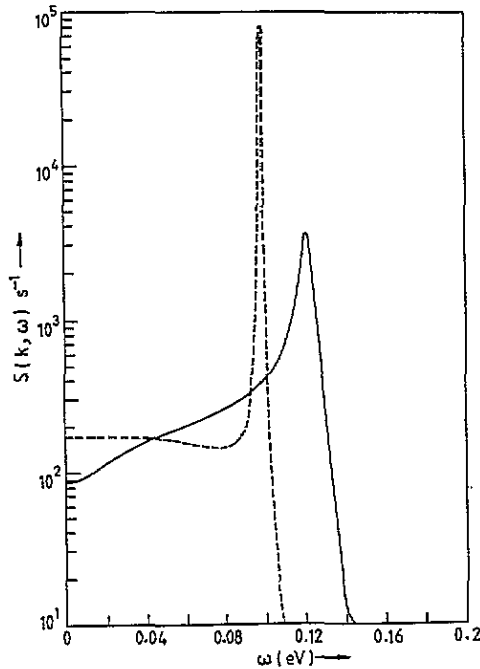


Figure 4. Dynamical structure factor $S(k, \omega)$ in the second inverse s^{-1} for the one-component rare hot plasma ($n = 3.9 \times 10^{18} \text{ cm}^{-3}$; $T = 297 \text{ K}$) for $k = 4.25 \times 10^6 \text{ cm}^{-1}$: - - -, when the plasma is considered to be classical; —, when the plasma is taken to be quantum.

this study is the same as in the earlier study, i.e. given by equation (18). The calculated values of $S^{cl.a}(k, \omega)$ (curves 3 and 4) together with $S^{cl}(k, \omega)$ (curves 1 and 2) are plotted in figure 5 for two values of k ($4.25 \times 10^6 \text{ cm}^{-1}$ and $6.2 \times 10^6 \text{ cm}^{-1}$).

In contrast with $S^{cl}(k, \omega)$ for a given k , $S^{cl.a}(k, \omega)$ has a zero value at $\omega = 0$, peaks at a lower energy, is broader and has a smaller value of the peak as is evident from figure 5. However, the static structure factors in the two cases are not very different from each other. For instance, for $k = 4.25 \times 10^6 \text{ cm}^{-1}$, $S^{cl.a}(k) = 0.066$ while $S^{cl}(k) = 0.061$. Thus, one concludes that $S^{cl}(k, \omega)$ is different from the corresponding $S^{cl.a}(k, \omega)$.

$S^{cl}(k, \omega)$ for different values of k have been computed and the different parameters such as the position of ω where the function peaks, its value, the full width at half-maximum, $S^{cl}(k, 0)$ and $S^{cl}(k)$ are determined. In figure 6 are plotted ω versus k results for the collective modes. For $k = 0$, $\omega = \omega_p (= 0.088 \text{ eV})$ which is the same as for the Drude model. As k increases to $k \simeq 1 \times 10^6 \text{ cm}^{-1}$, there is little increase in the value of ω . When $k > 1 \times 10^6 \text{ cm}^{-1}$, the increase in ω from ω_p becomes apparent and agrees with that given by the approximate $\varepsilon_1(k, \omega)$, i.e. equation (31) up to $k \simeq 2 \times 10^6 \text{ cm}^{-1}$. For $k > 2 \times 10^6 \text{ cm}^{-1}$ the difference between the collective modes given by the exact dielectric function and that given by the approximate dielectric function becomes noticeable. The position of the collective mode in the exact case is at a higher energy in comparison with that given by the approximate case, as is clear from the figure. In contrast, the Drude model yields the collective mode position to be at ω_p for all values of k . Thus, the present investigation gives a dispersion relationship different from both the Drude model as well as the approximate dielectric function of the hot plasma.

The positions of the full width at half-maximum have been plotted in figure 7(a) for

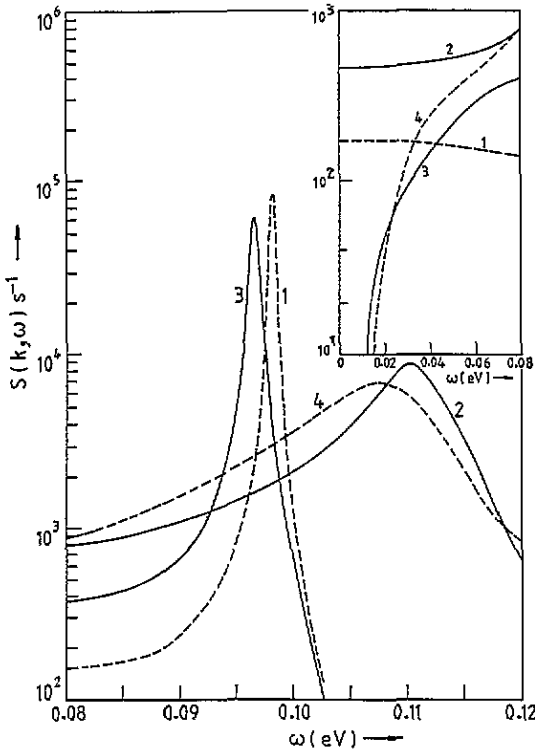


Figure 5. Comparison of dynamical structure factors for the OCCRHP ($n = 3.9 \times 10^{18} \text{ cm}^{-3}$; $T = 297 \text{ K}$). $S^{cl}(k, \omega)$ are computed from equation (17) with the approximate $S^{cl,a}(k, \omega)$ computed using equation (31) for the two values of k ($4.25 \times 10^6 \text{ cm}^{-1}$ and $6.0 \times 10^6 \text{ cm}^{-1}$). In the inset are shown the details of $S^{cl}(k, \omega)$ and $S^{cl,a}(k, \omega)$ for ω less than 0.08 eV. Curves 1 and 2 correspond to $S^{cl}(k, \omega)$ for $k = 4.25 \times 10^6 \text{ cm}^{-1}$ and $6.0 \times 10^6 \text{ cm}^{-1}$, respectively. Curves 3 and 4 correspond to $S^{cl,a}(k, \omega)$ for $k = 4.25 \times 10^6 \text{ cm}^{-1}$ and $6.0 \times 10^6 \text{ cm}^{-1}$, respectively.

different values of k . $S^{cl}(k, \omega)$ is an extremely sharp function for small values of k up to $k \simeq 2 \times 10^6 \text{ cm}^{-1}$ and therefore the damping is very small and hence the full width at half-maximum is nearly zero. As k increases, this width increases as shown in the figure.

In figure 7(b) are shown the values of the peaks of the collective modes for different values of k . As k increases, the peak values decrease and are quite different in the exact and approximate cases.

In figure 7(c) are shown $S^{cl}(k, 0)$; curve 2 is for different k . For $k \lesssim 1 \times 10^5 \text{ cm}^{-1}$, $S^{cl}(k, 0) = 0$ starts to increase slowly and then sharply as k increases as shown in the figure. $S^{cl,a}(k, 0)$ is zero for all values of k ! In the inset of figure 3 are shown the static structure factors $S(k)$ for different values of k . For $k = 0$, $S(k) = 0$ and increases mildly as k increases up to $k \simeq 1 \times 10^6 \text{ cm}^{-1}$ beyond which it increases perceptibly as is clear from the figure. $S^{cl,a}(k)$ are slightly different from the corresponding $S^{cl}(k)$ for different values of k as has also been noted earlier.

Strictly speaking, the system needs a quantum-mechanical description as λ_{rh} is comparable with the mean interparticle distance. Using the expression for $S^Q(k, \omega)$ given by equation (20), computations have been made. It may be emphasized that, for each k , the zeroth sum rule, i.e. $S^Q(k)$ from equation (24) and using equation (28) are the same. Similarly $S^Q(k, 0)$ from the calculated $S^Q(k, \omega = 0)$ and from equation (23) are also in

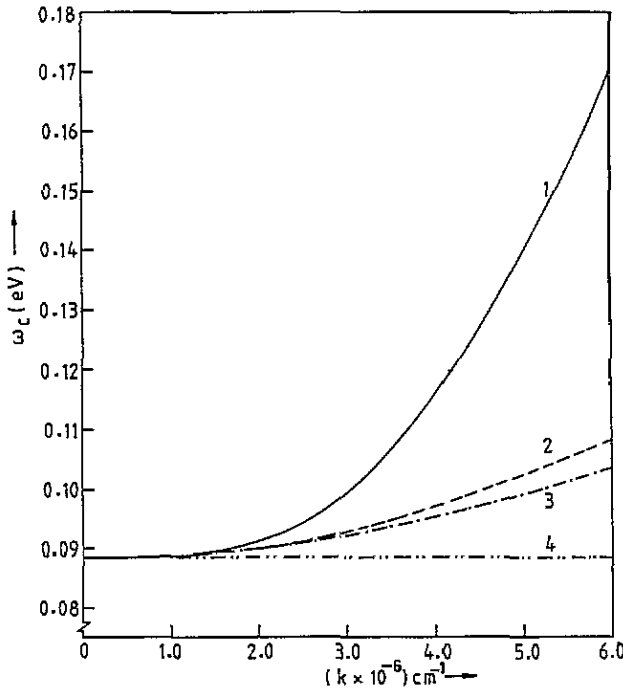


Figure 6. Variation in collective mode angular frequency ω_c with the wavevector k (i.e. dispersion relationship) for a one-component hot rare plasma ($n = 3.9 \times 10^{18} \text{ cm}^{-3}$; $T = 297 \text{ K}$) under different considerations: curve 1, quantum plasma (equation (10)); curve 2, classical plasma (equation (17)); curve 3, classical approximate plasma (equation (31)); line 4, classical plasma described by the Drude model (equation (33)).

agreement. Further, the collective mode determined by the value of ω at which the peak occurs and corresponding k have been used to evaluate $\varepsilon_1^Q(k, \omega)$ which turns out to be very close to zero, when $N = 100$. $S^Q(k, \omega)$ with ω for $k = 4.25 \times 10^6 \text{ cm}^{-1}$ is plotted in figure 4 for comparison with the corresponding classical case. $S^Q(k, \omega)$ peaks at a higher value of energy, is broader, is less peaked and has a lower value of $S^Q(k, 0)$ in comparison with the corresponding $S^{cl}(k, 0)$, as is clear from the figure.

Thus, the collective mode in the quantum-mechanical description of the system is not as well defined as in the classical case because of the broadening of the peak structure of $S^Q(k, \omega)$. The disorder in the system is substantially increased in comparison with that in the classical case.

In figure 6 are plotted the peak positions where the collective modes occur for different values of k . When k is small, the collective mode is present at the same frequency as in the classical case. When k becomes approximately equal to $1.5 \times 10^6 \text{ cm}^{-1}$, it starts to deviate and keeps increasing with increase in k as shown in the figure. For $k \approx 6 \times 10^6 \text{ cm}^{-1}$, the difference is quite large. Thus, the collective mode occurs at a higher energy in the quantum-mechanical case than in the corresponding classical case when k lies between, say, $2 \times 10^6 \text{ cm}^{-1}$ and $6 \times 10^6 \text{ cm}^{-1}$.

In figure 7(a) are plotted full widths at half-maximum for different values of k . The width in the quantum-mechanical case is more than in the corresponding classical case while this difference is small for small values of $k \leq 2 \times 10^6 \text{ cm}^{-1}$. It becomes significant with increase in the value of k as shown in the figure. It is a maximum for $k = 6 \times 10^6 \text{ cm}^{-1}$,

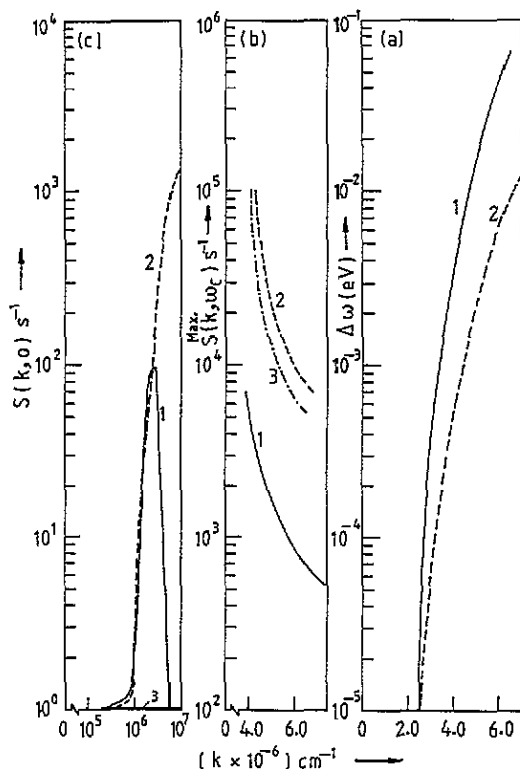


Figure 7. (a) Variation in the full width $\Delta\omega$ at half-maximum of the dynamical structure factor with wavevector k for the one-component rare hot plasma ($n = 3.9 \times 10^{18} \text{ cm}^{-3}$; $T = 297 \text{ K}$) under different conditions: curve 1, quantum plasma; curve 2, classical plasma; curve 3, classical approximate plasma. (b) Variation in the maximum value of the dynamical structure factor i.e. $S^{\text{max}}(k, \omega_c)$ with wavevector k for the one-component rare hot plasma ($n = 3.9 \times 10^{18} \text{ cm}^{-3}$; $T = 297 \text{ K}$) under different considerations: curve 1, quantum plasma; curve 2, classical plasma; curve 3, classical approximate plasma. (c) Variation in zero-frequency dynamical structure factor, i.e. $S(k, 0)$ with k for the one-component rare hot plasma ($n = 3.9 \times 10^{18} \text{ cm}^{-3}$; $T = 297 \text{ K}$) under different conditions: curve 1, quantum plasma; curve 2, classical plasma; x axis, i.e. $S(k) = 0$, classical approximate plasma.

the largest value of k considered here.

In figure 7(b) are plotted the values of peak of the collective modes, i.e. $S(k, \omega = \omega_c)$ for different k . In comparison with the corresponding classical values, $S^{\text{cl}}(k, \omega_c)$ peaks have lower values as shown in the figure.

In figure 7(c) are plotted $S^{\text{cl}}(k, 0)$ together with the classical result. For small k , the two are very close to each other and, even for larger k , the difference is not that significant as shown in the figure. Only when $k > 2 \times 10^6 \text{ cm}^{-1}$, does $S^{\text{cl}}(k, 0)$ show a sharp decrease and it continues for larger values of k .

In the inset of figure 3 are shown $S^{\text{cl}}(k)$ for k lying between 0 and $6 \times 10^6 \text{ cm}^{-1}$. For k between 0 and $2 \times 10^6 \text{ cm}^{-1}$, $S^{\text{cl}}(k)$ is close to $S^{\text{cl}}(k)$. For k greater than $2.5 \times 10^6 \text{ cm}^{-1}$, $S^{\text{cl}}(k)$ is less than $S^{\text{cl}}(k)$ as shown in the figure. For $k = 6 \times 10^6 \text{ cm}^{-1}$, the difference between $S^{\text{cl}}(k)$ and $S^{\text{cl}}(k)$ is a maximum.

4. Conclusions

Equations (11) and (16) are analytical expressions for $\varepsilon^Q(k, \omega)$ and $\varepsilon^{cl}(k, \omega)$ for the OCQRHP and the OCCRHP, respectively. These correctly describe the dynamics of the plasma for all values of wavevector and frequency.

The expression for the quantum-mechanical case, $\varepsilon_1^Q(k, \omega)$, is quite different from the corresponding classical expression $\varepsilon_1^{cl}(k, \omega)$. It reduces correctly to the classical case when $\hbar \rightarrow 0$ and gives quite a different dynamical description of the plasma when the quantum parameter $\hbar k/mV$ is large. This is reflected in the study of collective modes of the system which are quite different from the corresponding classical case, particularly for high values of the wavevector.

Equation (17) for $\varepsilon_1^{cl}(k, \omega)$ gives a very different result for larger values of ω/kV , in comparison with the approximate $\varepsilon_1^{cl,a}(k, \omega)$ used widely.

The effect of incorporating the quantum-mechanical nature of the plasma results in introducing a sort of disorder in the system (as exhibited by the broadening of the peak in the dynamical structure factor $S(k, \omega)$ of the plasma). This disorder increases with increase in the value of the wavevector.

It is clear from the study that for a thermal plasma the correct dielectric function is both k and ω dependent. It is, therefore, not quite correct to treat such a plasma using the Drude model [17] which is independent of the wavevector.

Acknowledgment

One of us (KB) gratefully acknowledges the financial assistance given by the UGC, New Delhi.

Appendix

Using the Green function formalism, the expression for the dielectric function $\varepsilon(k, \omega)$ for the strongly degenerate case can be written as follows [15]:

$$\varepsilon(k, \omega) = 1 + V(k)F^0(k, \omega + i\eta) \quad (\text{A1})$$

where

$$V(k) = 4\pi e^2/k^2$$

and

$$F^0(\bar{k}, \omega + i\eta) = -2 \int \frac{d^3\bar{p}}{(2\pi)^3} \frac{[n_{\bar{p}+\bar{k}}^0 - n_{\bar{k}}^0]}{(\hbar\omega + i\eta - \varepsilon_{\bar{p}+\bar{k}}^0 - \varepsilon_{\bar{k}}^0)} \quad (\text{A2a})$$

$$= F_1^0(\bar{k}, \omega) + iF_2^0(\bar{k}, \omega) \quad (\text{A2b})$$

where $n_{\bar{k}}^0$ and $n_{\bar{k}+\bar{p}}^0$ are the distribution functions at the momenta \bar{k} and $\bar{k} + \bar{p}$, respectively, and correspond to the Fermi-Dirac distribution functions.

In order to obtain $\varepsilon(k, \omega)$ for the OCQRHP, one has to substitute for $n_{\bar{k}}^0$ and $n_{\bar{k}+\bar{p}}^0$ in equation (A2a) the following expressions:

$$n_{\bar{k}}^0 = \exp(\beta u) \exp\left(-\frac{\beta \hbar^2 k^2}{2m}\right) \quad (\text{A3a})$$

and

$$n_{k+p}^0 = \exp(\beta u) \exp\left(-\frac{\beta \hbar^2 (k+p)^2}{2m}\right) \quad (\text{A3b})$$

where

$$\exp(\beta u) = \frac{1}{2} n \lambda_{rh}^3.$$

Using the Dirac identity given by equation (4) and simplifying, one can obtain the following expression for $F_2^0(k, \omega)$:

$$F_2^0(k, \omega) = \left(\frac{\pi}{2} \frac{m}{k_B T}\right)^{1/2} \frac{n}{\hbar k} \exp\left(-\frac{\hbar^2 k^2}{8mk_B T}\right) \exp\left(-\frac{m\omega^2}{2k^2 k_B T}\right) \\ \times \left[\exp\left(\frac{\hbar\omega}{2k_B T}\right) - \exp\left(-\frac{\hbar\omega}{2k_B T}\right) \right]. \quad (\text{A4})$$

Equation (A.4) is the same as equation (5).

One can obtain $F_1^0(k, \omega)$ after using the transformations

$$\omega' = \frac{kp}{m} \quad X^2 = \frac{\beta m}{2} \left(\frac{\omega'}{k} + \frac{\hbar k}{2m}\right)^2$$

and

$$Y^2 = \frac{\beta m}{2} \left(\frac{\omega}{k} + \frac{\hbar k}{2m}\right)^2 \quad (\text{A5})$$

and simplifying to get the following expression:

$$F_1^0(k, \omega) = \frac{1}{\sqrt{2\pi}} \left(\frac{m}{k_B T}\right)^{1/2} \frac{n}{\hbar k} \left\{ \int_{-\infty}^{\infty} \frac{dX}{Y-X} \exp\left[-\left(X + \frac{D}{2}\right)^2\right] \right. \\ \left. - \int_{-\infty}^{\infty} \frac{dX}{Y-X} \exp\left[-\left(X - \frac{D}{2}\right)^2\right] \right\}. \quad (\text{A6})$$

Equation (A6) can be transformed into the following expression:

$$F_1^0(k, \omega) = \left(\frac{m\beta}{2}\right)^{1/2} \frac{n}{\hbar k} \left[\Phi \left\{ \left(\frac{m\beta}{2}\right)^{1/2} \left(\frac{\omega}{k} + \frac{\hbar k}{2m}\right) \right\} - \Phi \left\{ \left(\frac{m\beta}{2}\right)^{1/2} \left(\frac{\omega}{k} - \frac{\hbar k}{2m}\right) \right\} \right] \quad (\text{A7})$$

with

$$\Phi(z) = \pi^{-1/2} P \int_{-\infty}^{\infty} dt \frac{\exp(-t^2)}{z-t}. \quad (\text{A8})$$

Equation (A7) is the same as equation (9). In the Green function formalism [15], only approximate expressions for $\Phi(z)$ have been obtained for $z \gg 1$ and $z \ll 1$.

While, $\Phi(z)$ is convergent for $z \ll 1$, it is divergent for $z \gg 1$. One can examine it by the ratio test. The ratio R of the n th to $(n-1)$ th terms of $\Phi(z)$ for $z \gg 1$ [15] is as follows:

$$R = \frac{n^2}{z^2} \left(2 - \frac{3}{n} + \frac{1}{n^2}\right). \quad (\text{A9})$$

In the limit $n \rightarrow \infty$, $R \rightarrow \infty$ and, therefore, the series diverges. Hence $\varepsilon_1(k, \omega)$ will also diverge. This is true for both the cases of z , i.e. z_+ and z_- given as

$$z_+ = \frac{\omega}{\sqrt{2kV}} + \frac{\hbar k}{2\sqrt{2mV}}$$

and

$$z_- = \frac{\omega}{\sqrt{2kV}} - \frac{\hbar k}{2\sqrt{2mV}}.$$

In $\varepsilon_1(k, \omega)$ calculations, the series containing z_- increases much more rapidly than that containing z_+ . The net result is a divergent $\varepsilon_1(k, \omega)$ which is an unphysical result. Such a situation does not occur for $z \ll 1$, and in this case $\varepsilon_1(k, \omega)$ is convergent.

The ratio R of the n th to $(n - 1)$ th terms in the series for $\varepsilon_1(k, \omega)$ in our expression given by equation (10) for both $z \gg 1$ and $z \ll 1$ is given as follows:

$$R = \frac{z^2 (2 - 1/n)}{n^2 (2 + 1/n)}. \quad (\text{A10})$$

For any z , as n tends to ∞ , $R \rightarrow 0$. This is true for both z_+ and z_- . We therefore obtain a convergent value of $\varepsilon_1(k, \omega)$ for all values of z .

We have also done explicit numerical calculations for various terms (i.e. n) for R , using equations (A9) and (A10) and the numbers do confirm the above results.

References

- [1] Dendy R O 1990 *Plasma Dynamics* (Oxford: Clarendon)
- [2] Ichimaru S 1992 *Statistical Plasma Physics* (Reading, MA: Addison-Wesley)
- [3] Biswas B and Tewari S P 1979 *J. Phys. C: Solid State Phys.* **12** L273
- [4] Tewari S P and Yadav P K 1976 *Phys. Lett.* **58A** 347
- [5] Biswas B and Tewari S P 1983 *J. Phys. C: Solid State Phys.* **16** 901
- [6] Ichimaru S 1962 *Ann. Phys., NY* **20** 78
- [7] Dandrea R G and Ashcroft N W 1986 *Phys. Rev. B* **34** 2097
Biswas B and Tewari S P 1980 *Phys. Rev. B* **22** 681
- [8] Gouedard C and Deutsch C 1978 *J. Math. Phys.* **19** 32
- [9] Pines D and Nozieres P 1966 *The Theory of Quantum Liquids I* (New York: Benjamin)
- [10] Sjolander A and Stott M J 1972 *Phys. Rev. B* **5** 2109
- [11] Trubnikov B A and Elesin V F 1965 *Soviet Phys.-JETP* **20** 866
- [12] Silin V P 1961 *Zh. Eksp. Teor. Fiz.* **40** 1768 (Engl. Transl. 1961 *Soviet Phys.-JETP* **13** 1244)
- [13] Tewari S P and Joshi H 1993 *Phys. Lett.* **173A** 160
- [14] Tewari S P and Joshi H 1995 *Pramana* **44** 271
- [15] Fetter A L and Walecka J D 1971 *Quantum Theory of Many Particle Systems* (New York: McGraw-Hill)
- [16] Grandy W T 1969 *J. Phys. Soc. Japan* **26** 82
- [17] Spitzer W G and Fan H Y 1957 *Phys. Rev.* **106** 882
- [18] Ashcroft N W and Mermin N D 1976 *Solid State Physics* (New York: Holt, Rinehart and Winston)
- [19] Rahman A 1973 *Phys. Rev. Lett.* **32** 52
Copley J R D and Rowe J M 1973 *Phys. Rev. Lett.* **32** 49
Tewari S P and Tewari S P 1978 *Phys. Lett.* **65A** 241